CSIRO PUBLISHING

RESEARCH FRONT

Environ. Chem. **2021**, *18*, 193–201
https://doi.org/10.1071/EN21003

DMS sea-to-air fluxes and their influence on sulfate aerosols over the Southern Ocean, south-east Indian Ocean and north-west Pacific Ocean

Miming Zhang,[A,E] *Christa A. Marandino,*[B] *Jinpei Yan,*[A] *Qi Lin,*[A] *Keyhong Park*[C] *and Guojie Xu*[D]

[A]Key Laboratory of Global change and Marine–Atmospheric Chemistry, Third Institute of Oceanography, Ministry of Natural Resource, Siming District, Xiamen, Fujian 361005, China.
[B]Forschungsbereich Marine Biogeochemie, GEOMAR Helmholtz Centre for Ocean Research, Düsternbrooker Weg 20, 24105 Kiel, Germany.
[C]Division of Polar Ocean Science, Korea Polar Research Institute, Incheon, 21990, South Korea.
[D]Collaborative Innovation Center on Forecast and Evaluation of Meteorological Disasters, Key Laboratory for Aerosol–Cloud–Precipitation of China Meteorological Administration, Nanjing University of Information Science and Technology, Nanjing 210044, China.
[E]Corresponding author. Email: zhangmiming@tio.org.cn

Environmental context. The ocean-produced dimethyl sulfide (DMS) molecule is thought to affect cloud formation and the solar radiation budget at the Earth's surface, hence playing an important role in regulating climate. In this study, we calculated the DMS sea-to-air flux across the Southern Ocean, south-east Indian Ocean and north-west Pacific Ocean, and analysed the influence of DMS fluxes on sulfate aerosols. These results improved our understanding of the effects of DMS emissions on sulfate compounds in the atmosphere over the global ocean.

Abstract. Oceanic dimethyl sulfide (DMS) is the most abundant biogenic sulfur compound emitted into the atmosphere and could indirectly regulate the global climate by impacting end product sulfate aerosols. DMS emissions and their influence on sulfate aerosols, i.e. methanesulfonic acid (MSA) and non-sea-salt sulfate (nss-SO_4^{2-}), were investigated over the Atlantic Ocean and Indian Ocean sectors of the Southern Ocean (SO), the south-east Indian Ocean, and the north-west Pacific Ocean from February to April 2014 during the 30th Chinese National Antarctic Research Expedition. We found a strong large-scale DMS source in the marginal sea ice zone from 34 °W to 14 °E of the SO (south of 60 °S), in which the mean flux was 49.0 ± 65.6 μmol m^{-2} d^{-1} (0.6–308.3 μmol m^{-2} d^{-1}, $n = 424$). We also found a second large-scale DMS source in the South Subtropical Front (~40 °S, up to 50.8 μmol m^{-2} d^{-1}). An inconsistency between concentrations of atmospheric sulfate compounds and DMS emissions along the cruise track was observed. The horizontal advection of air masses was likely the main reason for this discrepancy. Finally, the biological exposure calculation results also indicated that it is very difficult to observe a straightforward relationship between oceanic biomass and atmospheric MSA.

Keywords: dimethyl sulfide, DMS, sulfate aerosol, DMS sea-to-air fluxes, the Southern Ocean, Indian Ocean, Pacific Ocean, relationships.

Received 14 January 2021, accepted 7 April 2021, published online 30 April 2021

Introduction

Oceanic dimethyl sulfide (DMS) is an important climatically active biogenic gas, which is hypothesised to affect cloud condensation nuclei (CCN) and cloud formation and, thus, regulate Earth's climate by altering the atmospheric radiation budget (CLAW hypothesis, named after the first letters of authors' names) (Charlson et al. 1987; Vogt and Liss 2009). However, Quinn and Bates (2011) argued that oceanic biological DMS probably does not control CCN in the remote marine boundary layer, and that the major sources of CCN are likely sea salt particles and organics. Nonetheless, it has been observed that the oxides of DMS contribute to the sulfate aerosols in remote marine areas. Also, biogenic sulfur aerosols have been found to affect the microphysical and optical properties of clouds at mid and high latitudes (Gabric et al. 2005; Vallina et al. 2006; Lana et al. 2012). Additionally, DMS can be entrained in the stratosphere and contribute to sulfur loading in tropical regions (Marandino et al. 2013).

Methanesulfonic acid (MSA) and non-sea-salt sulfate (nss-SO_4^{2-}) are the two main by-products of DMS oxidation in the atmosphere (von Glasow and Crutzen 2004). MSA originates only from the oxidation of DMS and can be used as an indicator of marine biogenic sulfur production (Hezel et al. 2011). Considerable efforts have focussed on identifying and

quantifying the linkage between oceanic DMS emissions and CCN concentrations or atmospheric sulfur compounds (Ayers and Gras 1991; Ayers et al. 1991; Andreae and Crutzen 1997; Berresheim et al. 1998; Legrand et al. 2001; Preunkert et al. 2007; Preunkert et al. 2008). Indeed, the release of DMS from productive regions can strongly impact the atmospheric DMS mixing ratios in nearby regions (Park et al. 2013, 2018) and further impact sulfate aerosols (Park et al. 2017). However, the direct influence of oceanic DMS on sulfate aerosols over remote ocean areas is difficult to measure. Furthermore, atmospheric DMS levels in the marine boundary layer are not always consistent with seawater DMS values (Inomata et al. 2006; Marandino et al. 2013). The factors that contribute to sulfur loading in the marine boundary layer seem very complex, rather than driven only by DMS emissions.

It is challenging to obtain a comprehensive understanding of DMS emissions over the global ocean. In particular, the Southern Ocean (SO) has been estimated to contribute ~20 % of global annual DMS emissions (Lana et al. 2011); however, this value was possibly underestimated owing to the lack of field observation data (Levasseur 2011). The DMS emissions in the SO have been suggested to be very important to global climate because a CLAW-type feedback could help mitigate climate warming (Cameron-Smith et al. 2011; Levasseur 2011). Lana et al. (2011) reported that global DMS emissions were ~28.1 (17.6–34.4) Tg S based on a 3-fold increase in the amount of data (from 15 000 to 47 000 records in the NOAA–Pacific Marine Environmental Laboratory (PMEL) DMS database, http://saga.pmel.noaa.gov.dms), and the result was nearly 17 % higher than the estimation 10 years before (Kettle and Andreae 2000).

Strong seasonal variability of atmospheric sulfur compounds has been found at many research stations, such as the Cape Grim Baseline Air Pollution Station (40 °40.9′S, 144 °41.3′E) (Andreae et al. 1999), Amsterdam Island (37 °50′S, 77 °30′E) (Sciare et al. 2000), the Halley Station (75 °35′S, 26 °19′W) (Read et al. 2008), the Dumont d'Urville Station (66 °40′S, 140 °01′E) (Preunkert et al. 2007) and the Zhongshan Station (69 °22′S, 76 °22′W) (Zhang et al. 2015). In contrast, sulfate aerosol investigations in the marine boundary layer on board ships in the southern hemisphere oceans are insufficient and generally performed in the austral spring and summer seasons (Bates et al. 1992; Davison et al. 1996; Chen et al. 2012; Xu et al. 2013). Although high levels of sulfate aerosols have been observed during these cruises, identifying the origin of the atmospheric sulfur compounds is still ambiguous. This is difficult because of the lack of simultaneous high-resolution seawater and air DMS data, as well as that of the oxidation products, during the period under way. Studies comparing DMS emissions and sulfate aerosols along a cruise track are rare. Therefore, to improve on our previous studies (Chen et al. 2012; Xu et al. 2013) and further understand how DMS emissions influence sulfate aerosols in the southern hemisphere marine boundary layer, we performed continuous underway surface DMS measurements and bulk volume aerosol sampling, simultaneously, during the 30th Chinese National Antarctic Research Expedition (CHINARE – Ant) from February to April 2014.

Methods

Ship measurements

Our measurements were performed onboard the R/V *Xue Long* during the 30th CHINARE – Ant. The cruise track (Fig. 1) was described in detail in Zhang et al. (2017), and the study areas comprised two parts: Leg 1, named the west–east transect, from the Drake Passage to Prydz Bay, 7–24 February 2014; Leg 2, named the south–north transect, from Prydz Bay to Fremantle, Australia, 26 February–16 March 2014 and from Fremantle, Australia, to the East China Sea, 22 March–11 April 2014. According to the studies by Bates and Quinn (1997) and Curran and Jones (2000) and the observed surface water temperature and salinity, the transects were divided into five regions: (1) south of 58 °S, located in the seasonal ice zone (SIZ); (2) the region between 58 °S and 42 °S, located in the Subantarctic Zone and Antarctic Zone (SAAZ); (3) the region between 42 °S and 15 °S, located in the South Subtropical Zone (SSTZ); (4) the region between 15 °S and 15 °N, located in the equator region (EZ); (5) region to the north of 15 °N, located in the north Subtropical Zone (NSTZ).

The methodology for underway surface DMS measurements was described in detail in Zhang and Chen (2015) and Zhang

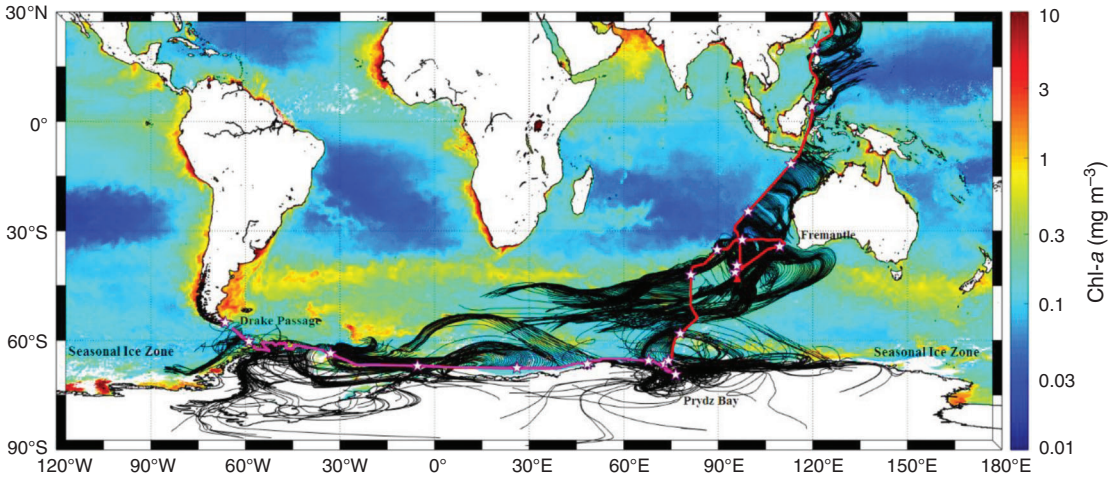

Fig. 1. Transect of the 30th CHINARE – Ant (purple, west–east transect; red, south–north transect). The black lines are the 5-day air mass back-trajectories every hour along the cruise track. The areas between the stars are the locations of bulk aerosol samples. The background is the monthly averaged Chl-*a* concentration (colour scale), and the white represent areas where Chl-*a* is undetectable.

et al. (2017). A DMS sample was collected every 10 min with a detection limit of 0.05 nM. The measurements of other parameters, such as sea surface temperature (SST), sea surface salinity (SSS), wind speed, air pressure, sea ice concentration and remote-sensing chlorophyll *a* (Chl-*a*) data, were also described in Zhang et al. (2017). A total of 20 bulk aerosol samples were collected with a sampling interval of 2 or 3 days (Fig. 1; the detailed information of the aerosol sample locations is shown in Table S1, Supplementary material). The details of the sampling and analysis methods of aerosols were the same as those in Chen et al. (2012) and Zhang et al. (2015). The concentrations of nss-SO_4^{2-} were calculated with the equation: $[\text{nss-}SO_4^{2-}] = [SO_4^{2-}]_{\text{total}} - 0.252[Na^+]$, where 0.252 is the mass ratio of SO_4^{2-}/Na^+ in bulk seawater (Millero and Sohn 1992).

The calculation of sea-to-air DMS fluxes

Ocean–atmosphere DMS fluxes are computed using the following gas exchange model:

$$F = k_T\left(C_w - C_g/H\right) \quad (1)$$

where k_T is the transfer velocity; C_w and C_g are the DMS concentrations in seawater and the atmosphere, respectively; H is the solubility of gas in seawater. There is evidence to suggest that the DMS flux calculation result could be significantly influenced by atmospheric DMS, which could add up to 17 % uncertainty (Lennartz et al. 2015). However, in order to compare with the calculation results of Lana et al. (2011), and because atmospheric DMS concentrations are generally far less than the concentration in seawater, we neglected the atmospheric DMS contribution in the DMS sea-to-air calculation as in Eqn 1. The k_T is parameterised with the wind speed and the most widely used equations are from Liss and Merlivat (1986) (hereafter LM86), Wanninkhof (1992) (hereafter W92) and Nightingale et al. (2000) (hereafter N00). However, the results of the flux calculations would differ when using different equations (Table 1). To compare our calculation results with those in Lana et al. (2011), we decided to use the equation N00 as follows for the discussion:

$$\text{N00}: k_T = \left(0.222\,U_{10}{}^2 + 0.333\,U_{10}\right)\left(Sc_{DMS}/600\right)^{-1/2} \quad (2)$$

where Sc_{DMS} (Schmidt number of DMS) is a function of SST according to Saltzman et al. (1993); 600 is the Schmidt number of CO_2 in fresh water at 25 °C and 35 psu; U_{10} is the 10-m wind speed. As the height of the wind speed measurements on the ship is ~27 m, we calibrated the wind speed to that at 10 m as in Hsu et al. (1994) as follows:

$$U_x/U_{10} = (Z_x/Z_{10})^p \quad (3)$$

where U_{10} is the wind speed at a height of 10 m, U_x is the observed wind speed at 27 m, Z_x and Z_{10} are 27 and 10 m, respectively, and the p value is 0.11, as referred to in Hsu et al. (1994).

The calculation of biological exposure to oceanic chlorophyll along the trajectories

We performed a 5-day air mass back-trajectory along the cruise track every hour using the hybrid single-particle Lagrangian integrated 97 trajectories (HYSPLIT) model (Fig. 1). Similarly to the method reported by Arnold et al. (2010), back-trajectory position and satellite Chl-*a* data are combined to yield time-series parameters along the cruise ship track based on the sea surface Chl-*a* 'fetch' of arriving air masses. The first parameter, the average (Avg) chlorophyll exposure, which is the mean of the marine Chl-*a* concentrations taken from Sea-WiFS data at the 6-hourly positions along the length of the back-trajectory, was calculated. The second parameter, the integrated (Int) chlorophyll exposure or age-weighted chlorophyll exposure (*Ea*), was also calculated by applying an e-folding lifetime of 5 days to each Chl-*a* value included in the average with time backward along each back-trajectory, as described in Arnold et al. (2010):

$$Ea = \frac{\sum_i [\text{Chl-}a]_i \exp(t_i/5)}{n} \quad (4)$$

where $[\text{Chl-}a]_i$ and t_i are the ocean Chl-*a* concentrations and the time in days before arrival at the ship position at each point along the back-trajectory, respectively, and n is the total number of time points with valid Chl-*a* values included in the calculation. The Chl-*a* data are the 8-day mean Chl-*a* concentrations from

Table 1. Mean DMS concentrations, sea-to-air DMS fluxes (from various parameterisations) and wind speeds in distinct ocean regions
Note that the ranges are given under the mean values. n.d. means the values were under the detection limit

Regions	Month		DMS (nM)	Wind speed (m s^{-1})	DMS flux (μmol m^{-2} d^{-1})		
					LM86	W92	N00
South of 58 °S SIZ	Feb	Mean	4.1 ± 8.3	8.8 ± 4.1	9.7 ± 24.5	10.1 ± 26.8	13.9 ± 36.2
		Range	0.1–73.2	0.2–23.1	n.d.–205.3	n.d.–228.8	n.d.–308.3
		Number	2155	1951	1941	1941	1941
58 °S to ~42 °S SAAZ	Mar	Mean	2.4 ± 1.5	10.9 ± 3.9	7.9 ± 6.4	10.9 ± 9.7	11.1 ± 9.1
		Range	0.5–9.6	2.0–18.7	n.d.–37.0	0.1–53.8	0.2–50.8
		Number	724	722	720	720	720
42 °S to ~15 °S SSTZ	Mar	Mean	3.1 ± 1.8	6.6 ± 3.0	4.8 ± 4.5	7.7 ± 6.6	6.9 ± 5.9
		Range	0.5–9.9	0.8–19.00	0.1–26.6	0.1–43.0	0.2–38.8
		Number	1879	1795	1792	1792	1792
15 °S to ~15 °N EQ	Apr	Mean	2.4 ± 0.9	4.7 ± 2.2	2.5 ± 2.5	5.6 ± 4.5	4.1 ± 3.1
		Range	0.9–6.9	0.5–9.8	n.d.–17.5	n.d.–34.8	0.1–23.6
		Number	762	721	721	721	721
North of 15 °N NSTZ	Apr	Mean	2.2 ± 1.8	4.2 ± 1.8	1.7 ± 2.0	3.5 ± 3.2	2.9 ± 2.7
		Range	0.9–16.9	0.5–8.8	n.d.–12.8	n.d.–19.8	n.d.–19.7
		Number	395	395	395	395	395

the level 3 product of Sea-WiFS data at 4-km resolution. Missing data in the 8-day average satellite fields are replaced by values from available monthly mean satellite data. If the pressure of the air mass is lower than 850 hPa at the evaluated time points, a zero Chl-*a* value is included in the average (and integration). Time periods for which Chl-*a* data are missing for more than 50 % of the back-trajectory time points over the 5 days before ship arrival are excluded from the analysis. A zero Chl-*a* value was assigned to the time points for which the air mass passed over the land and sea ice region. The trajectory time points where there are missing satellite data over the ocean are excluded from the calculation.

Results and discussion

Computed DMS sea-to-air fluxes along the transects

In the west–east transect, the computed DMS sea-to-air fluxes, which had a mean value of 18.1 ± 42.0 μmol m^{-2} d^{-1} (d, day; ranging from 0.1 to 308.3 μmol m^{-2} d^{-1}, $n = 1387$), coincided with the variation in surface seawater DMS concentrations (ranging from 0.1 to 73.2 nM (mean value was 5.0 ± 9.7 nM); Fig. 2)). Obviously, we found significant sources of oceanic DMS along the marginal sea ice zone located from 34 °W to 14 °E (Zhang et al. 2017; see the data between the yellow lines in Fig. 2), and the mean DMS flux was 49.0 ± 65.6 μmol m^{-2} d^{-1} (ranging from 0.6 to 308.3 μmol m^{-2} d^{-1}, $n = 424$). The DMS source location was slightly east of that in Lana et al. (2011). The mean DMS flux value was much higher than that in previous studies over the polynyas in spring (20 ± 20 μmol m^{-2} d^{-1}, 11 November–4 December 2006, Ross Sea; Tortell et al. 2011) and summer (23.1 μmol m^{-2} d^{-1}, 11 January 2006–16 February 2009, Amundsen Sea; Tortell et al. 2012; 40 ± 30 μmol m^{-2} d^{-1}, 26 December 2005–24 January 2006, Ross Sea; Tortell et al. 2011), but lower than those measured in the study by Kim et al. (2017) (85 ± 119 μmol m^{-2} d^{-1}, 16 January–11 February 2016, Amundsen Sea).

In the south–north transect, as seen in Fig. 3, the mean DMS value was 6.3 ± 6.3 μmol m^{-2} d^{-1} (ranging from not detected (n.d.) to 50.8 μmol m^{-2} d^{-1}, $n = 4182$). Notably, a large-scale DMS source with a mean flux of 11.6 ± 8.4 μmol m^{-2} d^{-1} (ranging from 0.3 to 50.8 μmol m^{-2} d^{-1}, $n = 1164$) was demonstrated around the region (44 °S–34 °S, 81 °E–104 °E) located in the South Subtropical Front (~40 °S). High DMS concentrations at ~40 °S were also found by Chuck et al. (2005), and our calculated DMS sea-to-air mean flux over this range was in agreement with the results in Lana et al. (2011).

We compared the DMS sea-to-air flux values in distinct regions (Table 1). Significant DMS sources were found in the southern hemisphere. The highest mean DMS emission was found in the SIZ, 13.9 ± 36.2 μmol m^{-2} d^{-1} (n.d.–308.3 μmol m^{-2} d^{-1}, $n = 1941$). This result could be attributed to the high DMS levels (4.1 ± 8.3 nM) and relatively high wind speeds (mean value 8.8 ± 4.1 m s^{-1}) in this area. Owing to the strong spatial and temporal variability of surface seawater DMS over the SO (Tortell and Long 2009), the accuracy of the DMS emission evaluations depends on the understanding of the DMS distribution climatology. In the case of the SAAZ, the average flux values ranged from 7.9 to 11.1 μmol m^{-2} d^{-1} (Table 1, using the LM86, W92 and N00 parameterisations). The results were all much higher than those estimated by Curran and Jones (2000) in springtime at SAZ (3.8 μmol m^{-2} d^{-1}), AZ (1.7 μmol m^{-2} d^{-1}) and in summer at SAZ (6.7 μmol m^{-2} d^{-1}), respectively (by LM86). Moreover, there was no significant deviation in the DMS mean flux values between the SIZ and SAAZ (~3 μmol m^{-2} d^{-1}), which was

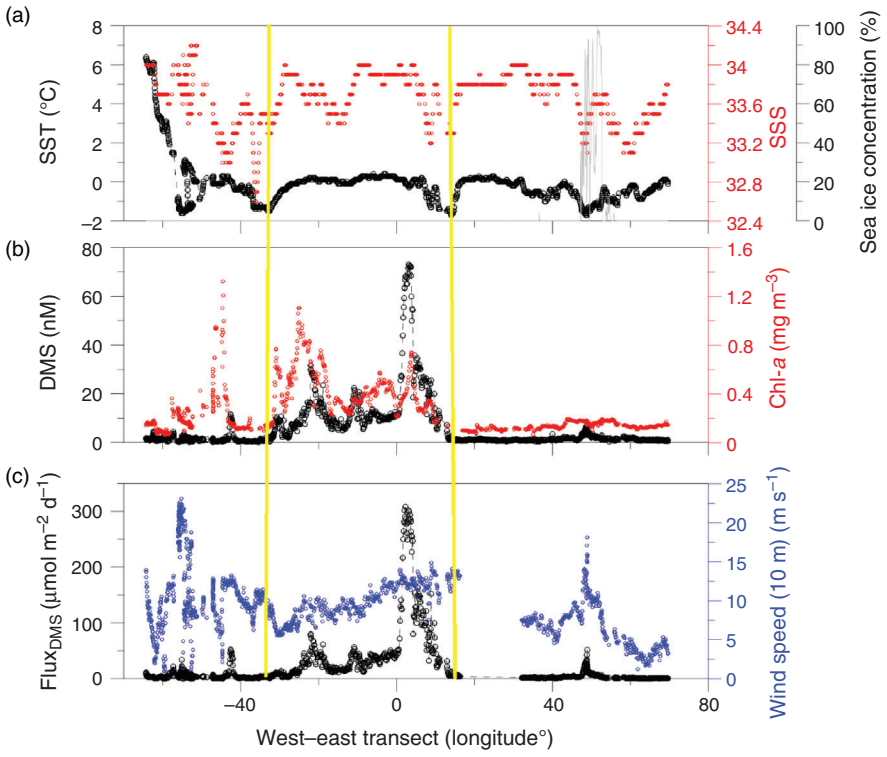

Fig. 2. DMS concentrations and sea-to-air flux along the west-east transect: (a) SST (black), SSS (red), and sea ice concentrations (grey); (b) DMS concentrations (black) and monthly average Chl-*a* (red); (c) DMS sea-to-air flux (black) and wind speed (blue).

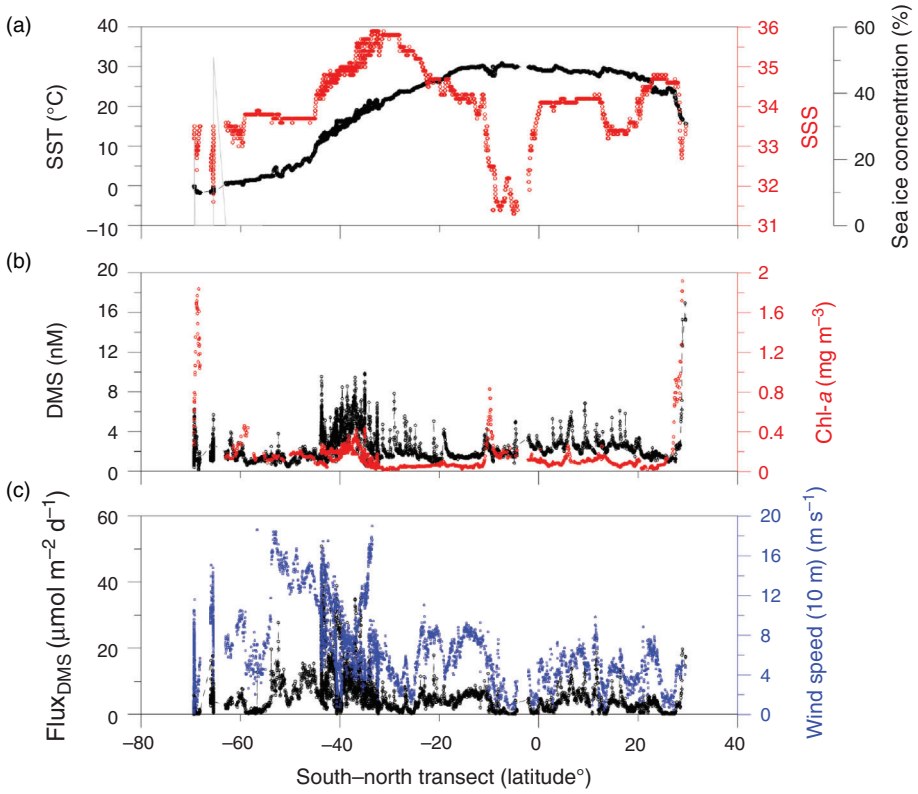

Fig. 3. DMS concentrations and sea-to-air flux in the south-north transect: (a) SST (black), SSS (red), and sea ice concentrations (grey line); (b) DMS concentrations (black) and 8-day average Chl-*a* (red); (c) DMS sea-to-air flux (black) and wind speed (blue).

different from the results of Curran and Jones (2000) (greater than 29 μmol m^{-2} d^{-1} in the summer). Our investigation indicated that the DMS emissions in the SAAZ were significant and comparable with those in the SIZ in March (sampling time). Thus, attention should be paid to the SAAZ when evaluating the global DMS emissions estimated by Lana et al. (2011). We also found relatively high DMS emissions in the SSTZ, which can be attributed to the significant DMS levels in the Subtropical Front. In contrast, the mean DMS fluxes were lowest in the EZ, 4.1 ± 3.1 μmol m^{-2} d^{-1} (0.1–23.6 μmol m^{-2} d^{-1}), and NSTZ, 2.9 ± 2.7 μmol m^{-2} d^{-1} (n.d.–19.7 μmol m^{-2} d^{-1}) during the observations. However, as seen in Fig. 3, the calculated DMS fluxes from low-latitude regions were much lower than the reports from the similar areas of the Chinese marginal sea, such as in the East China Sea (18.64 ± 14.92 μmol m^{-2} d^{-1}) (Zhai et al. 2019) and northern South China Sea (15.6 ± 11.6 μmol m^{-2} d^{-1}) (Zhai et al. 2020).

Influence of DMS emission on sulfur aerosols

The atmospheric sulfur compounds MSA and nss-SO_4^{2-} were detected during the CHINARE expedition. The mean values of MSA and nss-SO_4^{2-} were 64.03 ± 40.41 ng m^{-3} (11.08–162.19 ng m^{-3}) and 983.60 ± 1974.42 ng m^{-3} (n.d.–8695.94 ng m^{-3}), respectively. Similarly to our previous studies (Chen et al. 2012; Xu et al. 2013), high MSA levels were generally found in the SO (Fig. 4), which was consistent with the high DMS emissions in the SO. Additionally, the high MSA concentrations are also related to the low air temperature in the SO, as low temperatures are beneficial for the production of MSA from DMS oxidation (Bates et al. 1992). Extremely high nss-SO_4^{2-} concentrations were observed in the northern hemisphere, especially for the observations in the East China Sea (>2000 ng m^{-3}), due to the input of massive amounts of anthropogenic SO_2 (Yang et al. 2009).

However, the MSA distribution pattern was not coincident with the DMS changes and strengthened emissions (Fig. 4). For example, the lowest MSA value (16.16 ng m^{-3}) in the west–east transect from 35 ° to 5 °W corresponded to the relatively high average DMS values and fluxes of 9.7 ± 6.1 nM and 16.1 ± 12.2 μmol m^{-2} d^{-1}, respectively. Conversely, the highest MSA concentration (162.19 ng m^{-3}) was associated with a relatively low DMS average value of 1.3 ± 1.3 nM and a flux of 3.3 ± 4.2 μmol m^{-2} d^{-1}. Even in the high-DMS source waters, for example from 5 °W to 26 °E, the average DMS value was 14.2 ± 18.9 nM, and the flux was 59.5 ± 58.4 μmol m^{-2} d^{-1}; only moderate MSA and nss-SO_4^{2-} concentrations of 77.80 and 95.24 ng m^{-3}, respectively, were observed. Additionally, in the Subtropical Front region (~40 °S), relatively high DMS emissions (18.2 ± 9.2 μmol m^{-2} d^{-1}) with high wind speeds (10.9 ± 2.7 m s^{-1}) were found, corresponding to relatively low MSA and nss-SO_4^{2-} concentrations of 23.85 and 138.62 ng m^{-3}, respectively. It is well known that the DMS conversion to aerosol precursors is not instantaneous (DMS lifetime is ~1 day; Kloster et al. 2006). The time lag and air mass transportation are possible significant factors in the inconsistency between DMS fluxes and sulfate aerosol concentrations. On the other hand, our recent study indicated that gaseous MSA contributed almost 31 % of the total MSA (Yan et al. 2019), while our results were only able to show particle MSA. This may also be a factor in the discrepancy between DMS flux and sulfate aerosol.

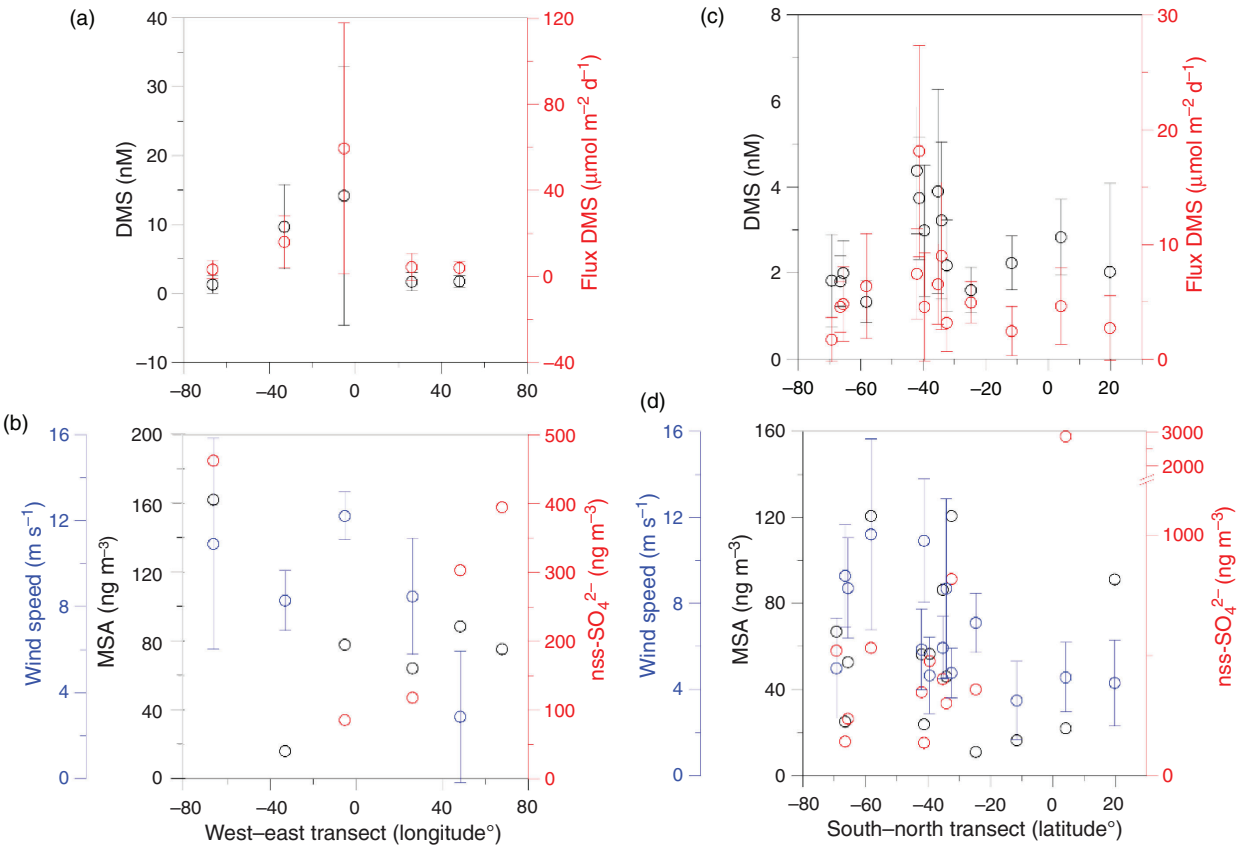

Fig. 4. The distributions of the sulfur aerosol and DMS emissions. Average seawater DMS concentrations (black) and sea-to-air fluxes (red) along the (a) west–east transect, and (c) south–north transect; average wind speed (blue), MSA (black) and nss-SO_4^{2-} (red) concentrations along the (b) west–east transect, and (d) south–north transect. The DMS, DMS flux and wind speed data are averaged over the aerosol sampling interval period (~3 days).

We noticed the horizontal mixing of air masses to be one of the critical factors based on the results of the 5-day air mass back-trajectories along the cruise track (Fig. 1). As the lifetime of sulfate aerosols is longer than 3 days (Kloster et al. 2006), under high wind speeds, especially in the SO (Fig. 4c, d), the air masses from other regions can impact the air masses of the sampling area and cause discrepancies between the oceanic DMS sources and atmospheric sulfur compounds. On the other hand, a previous study by Marandino et al. (2013) reported that the atmospheric DMS concentration is likely influenced by horizontal air mass advection rather than by in situ fluxes. In addition, the lifetime of DMS in the atmosphere is generally 1 day (Read et al. 2008) and can possibly be as long as 2–7 days under low air temperature conditions (Berresheim 1987). Therefore, the DMS released from remote regions can be quickly transported to other areas under high wind speeds (>10 m s^{-1}), which could also be one of the reasons for the observed discrepancy. Compared with research at a fixed sampling site, such as the Zhongshan Station (Zhang et al. 2015), in which the variations in sulfur aerosols were easily linked to local phytoplankton activity, a study along a moving cruise track should consider the rapid transport of air masses to better understand how remote oceanic DMS impacts sulfur compounds. Additionally, we noticed that the large difference in air temperature between the distinct regions could possibly influence the DMS lifetime (Atkinson et al. 2004). The DMS lifetime in low-latitude regions could have been shorter than that in the high-latitude regions because of the higher tropical temperatures. This would result in greater transport potential at high latitudes than in the more temperate regions.

Biological exposure calculation and its influence on sulfate aerosols

We also performed the calculation described in *Methods*, and the calculation results were compared with the measured MSA concentrations (Table 2). Similar to the study by Park et al. (2018), the calculated average or integrated chlorophyll exposure is assumed to be a good proxy for biomass and DMS sources (see empirical equation in Simo and Dachs 2002)). Additionally, we assumed that oceanic DMS could be directly emitted into the air and converted into sulfur compounds along the trajectories. However, we found that there was no significant relationship between the calculated Chl-*a* (Avg) and Chl-*a* (Int) values and MSA. This result could be explained by the production of MSA from DMS oxidation, which is related to temperature (Lin et al. 2012) and other parameters, such as light intensity (radical activity) and condensation sink (von Glasow and Crutzen 2004). Therefore, it might be difficult to find a straightforward relationship between oceanic biomass (biological exposure) and MSA in the atmosphere with a limited amount of data (only 20 records in the present study), even when potential large-scale influence is taken into consideration.

On the other hand, as DMS oxidation is the only source of MSA, it is possible that the MSA to Chl-*a* exposure ratio could be used to further investigate the oceanic DMS production

Table 2. Comparison of biological exposure with MSA levels

Regions	Sample no.	Chl-*a* (Avg) ($mg\,m^{-3}$)	Chl-*a* (*Ea*) ($mg\,m^{-3}$)	DMS (Avg) ($nmol\,L^{-1}$)	MSA ($ng\,m^{-3}$)	MSA/Chl-*a* (Avg)	MSA/Chl-*a* (Int)
SIZ	NJ30-31	0.27	31.08	6.62	16.16	58.96	0.52
	NJ30-32	0.28	32.64	17.30	77.80	281.30	2.38
	NJ30-33	0.26	30.90	1.54	64.31	247.80	2.08
	NJ30-34	0.14	15.02	2.32	88.48	636.62	5.89
	NJ30-35	0.11	13.17	1.18	75.37	690.15	5.72
	NJ30-36	0.12	14.28	1.87	67.03	550.17	4.70
	NJ30-37	0.10	12.50	1.62	25.12	260.77	2.01
	NJ30-38	0.10	14.02	2.11	52.78	525.91	3.76
	NJ30-39	0.16	18.95	1.34	120.64	764.48	6.37
	Total (Avg)	0.17	20.28	3.99	65.30	446.24	3.72
SAAZ	NJ30-30	0.11	12.66	1.27	162.19	1501.14	12.81
	NJ30-40	0.22	26.06	3.66	56.42	259.97	2.17
	Total (Avg)	0.16	19.36	2.47	109.31	880.56	7.49
SSTZ	NJ30-41	0.19	23.11	4.68	86.33	448.22	3.74
	NJ30-42	0.18	21.09	2.13	120.58	688.40	5.72
	NJ30-43	0.20	24.13	3.18	46.11	229.56	1.91
	NJ30-44	0.20	23.81	3.63	23.85	120.29	1.00
	NJ30-45	0.14	17.05	3.36	56.64	398.74	3.32
	NJ30-46	0.14	17.12	1.71	11.08	77.85	0.65
	Total (Avg)	0.18	21.05	3.11	57.43	327.18	2.72
EZ	NJ30-47	0.18	21.52	2.09	16.42	91.25	0.76
	NJ30-48	0.11	12.59	2.81	21.94	208.56	1.74
	Total (Avg)	0.14	17.06	2.45	19.18	149.91	1.25
NSTZ	NJ30-49	0.50	59.33	2.55	91.23	183.02	1.54

capacity (Table 2). The calculated Chl-*a* (Avg), Chl-*a* (Int) and MSA to Chl-*a* exposure ratio varied greatly. In general, the MSA to Chl-*a* exposure ratios of the aerosol samples collected in the regions of the Antarctic Ocean (both SIZ and SAAZ) were greater than the values collected in the mid-latitude and subtropical regions. The highest MSA to Chl-*a* exposure ratio was observed for the aerosol sample taken at site NJ-30-30, which is where the research vessel passed over the SAAZ region. However, it was not easy to simply compare the relative strength of the DMS sources between the SIZ and SAAZ because only two aerosol samples were collected in the SAAZ. Therefore, we conclude that the DMS production capacity of the Antarctic Ocean was greater than that of the mid-latitude and subtropical water, as indicated by the MSA to Chl-*a* exposure ratio. The calculation results were consistent with our measurements of surface water DMS levels along the transects, in which high levels of DMS generally occurred in high-latitude regions.

Conclusion

During the 30th CHINARE – Ant from February to April 2014, high-resolution shipboard measurements of surface water DMS were collected. We found two significant DMS sources: one was located in the marginal sea ice zone of the SO from 34 °W to 14 °E, where the mean DMS flux was $49.0 \pm 65.6\ \mu mol\,m^{-2}\,d^{-1}$ (0.6–308.3 $\mu mol\,m^{-2}\,d^{-1}$, $n = 424$); the other was located in the South Subtropical Front (~40 °S), where the mean DMS flux was $11.6 \pm 8.4\ \mu mol\,m^{-2}\,d^{-1}$ (ranging from 0.3 to 50.8 $\mu mol\,m^{-2}\,d^{-1}$, $n = 1164$). The high-resolution measurements of surface DMS greatly improved the estimation of DMS emissions, especially in the SO, where strong spatial and temporal variability of the seawater DMS levels on a small scale (<1 km) was found (Tortell and Long 2009). We also found inconsistencies between atmospheric sulfate compounds and DMS emissions along the transects. This result could be attributed to the horizontal advection of air masses, which would possibly impact atmospheric sulfate compounds, including MSA, nss-SO_4^{2-} and DMS, over the sampling sites. The biological exposure calculation results also indicated that it might be difficult to find a straightforward relationship between oceanic biomass and MSA over the maritime environment. Additionally, the MSA to Chl-*a* exposure ratio results demonstrated that the DMS production capacity of the Antarctic Ocean was greater than that of the mid-latitude and subtropical water.

Supplementary material

The locations of aerosol samples (Table S1) are available on the Journal's website.

Conflicts of interest

The authors declare no conflicts of interest.

Declaration of funding

This work was supported by the National Natural Science Foundation of China (NSFC) (4207060283, 41911540471), the Scientific Research Foundation of the Third Institute of Oceanography, at the Ministry of Natural Resources (under contracts no. 2019009, 2019008, 2018014), the international cooperation program managed by the National Research Foundation of Korea (NRF-2019K2A9A2A06025329), funding from the International Organizations and Conference and Bilateral Cooperation of Maritime Affairs, Ministry of Science and Technology and Key Research and Development Programs No. 2018YFC1406703, the International Organizations and Conference and Bilateral Cooperation of Maritime Affairs, the Chinese Projects for Investigations and Assessments of the Arctic and Antarctic (CHINARE2017–2020), the fund of China

Scholarship Council and the Korean Polar Research Institute (Grant PE21110).

Acknowledgements

We thank the Chinese Arctic and Antarctic Administration (CAA) of the State Oceanic Administration (SOA) and the crew of R/V *Xue Long* for support with field operations. We thank Professor Dr Ki-tae Park from the Korea Polar Research Institute for helping us to calculate biological exposure.

References

Andreae MO, Crutzen PJ (1997). Atmospheric aerosols: biogeochemical sources and role in atmospheric chemistry. *Science* **276**, 1052–1058. doi:10.1126/SCIENCE.276.5315.1052

Andreae MO, Elbert W, Cai Y, Andreae TW, Gras J (1999). Non-sea-salt sulfate, methanesulfonate, and nitrate aerosol concentrations and size distributions at Cape Grim, Tasmania. *Journal of Geophysical Research* **104**, 21695–21706. doi:10.1029/1999JD900283

Arnold SR, Spracklen DV, Gebhardt S, Custer T, Williams J, Peeken I, Alvain S (2010). Relationships between atmospheric organic compounds and air-mass exposure to marine biology. *Environmental Chemistry* **7**, 232–241. doi:10.1071/EN09144

Atkinson R, Baulch DL, Cox RA, Crowley JN, Hampson RF, Hynes RG, Jenkin ME, Rossi MJ, Troe J (2004). Evaluated kinetic and photochemical data for atmospheric chemistry: Volume I – gas phase reactions of O_x, HO_x, NO_x and SO_x species. *Atmospheric Chemistry and Physics* **4**, 1461–1738. doi:10.5194/ACP-4-1461-2004

Ayers G, Gras J (1991). Seasonal relationship between cloud condensation nuclei and aerosol methanesulphonate in marine air. *Nature* **353**, 834–835. doi:10.1038/353834A0

Ayers G, Ivey J, Gillett R (1991). Coherence between seasonal cycles of dimethyl sulphide, methanesulphonate and sulphate in marine air. *Nature* **349**, 404–406. doi:10.1038/349404A0

Bates TS, Quinn PK (1997). Dimethylsulfide (DMS) in the equatorial Pacific Ocean (1982 to 1996): evidence of a climate feedback? *Geophysical Research Letters* **24**, 861–864. doi:10.1029/97GL00784

Bates TS, Calhoun JA, Quinn PK (1992). Variations in the methanesulfonate to sulfate molar ratio in submicrometer marine aerosol particles over the South Pacific Ocean. *Journal of Geophysical Research* **97**, 9859–9865. doi:10.1029/92JD00411

Berresheim H (1987). Biogenic sulfur emissions from the Subantarctic and Antarctic Oceans. *Journal of Geophysical Research* **92**, 13245–13262. doi:10.1029/JD092ID11P13245

Berresheim H, Huey JW, Thorn RP, Eisele FL, Tanner DJ, Jefferson A (1998). Measurements of dimethyl sulfide, dimethyl sulfoxide, dimethyl sulfone, and aerosol ions at Palmer Station, Antarctica. *Journal of Geophysical Research* **103**, 1629–1637. doi:10.1029/97JD00695

Cameron-Smith P, Elliott S, Maltrud M, Erickson D, Wingenter O (2011). Changes in dimethyl sulfide oceanic distribution due to climate change. *Geophysical Research Letters* **38**, L07704. doi:10.1029/2011GL047069

Charlson RJ, Lovelock JE, Andreaei MO, Warren SG (1987). Oceanic phytoplankton, atmospheric sulphur, cloud. *Nature* **326**, 655–661. doi:10.1038/326655A0

Chen L, Wang J, Gao Y, Xu G, Yang X, Lin Q, Zhang Y (2012). Latitudinal distributions of atmospheric MSA and MSA/nss-SO_4^{2-} ratios in summer over the high latitude regions of the southern and northern hemispheres. *Journal of Geophysical Research* **117**, D10306. doi:10.1029/2011JD016559

Chuck AL, Turner SM, Liss PS (2005). Oceanic distributions and air-sea fluxes of biogenic halocarbons in the open ocean. *Journal of Geophysical Research* **110**, C10022. doi:10.1029/2004JC002741

Curran MAJ, Jones GB (2000). Dimethyl sulfide in the Southern Ocean: seasonality and flux. *Journal of Geophysical Research* **105**, 20451–20459. doi:10.1029/2000JD900176

Davison B, O'Dowd C, Hewitt CN, Smith M, Harrison RM, Peel D, Wolf E, Mulvaney R, Schwikowski M, Baltenspergert U (1996). Dimethyl sulfide and its oxidation products in the atmosphere of the Atlantic and Southern Oceans. *Atmospheric Environment* **30**, 1895–1906. doi:10.1016/1352-2310(95)00428-9

Gabric AJ, Shephard JM, Knight JM, Jones G, Trevena AJ (2005). Correlations between the satellite-derived seasonal cycles of phytoplankton biomass and aerosol optical depth in the Southern Ocean: evidence for the influence of sea ice. *Global Biogeochemical Cycles* **19**, GB4018. doi:10.1029/2005GB002546

Hezel P, Alexander B, Bitz C, Steig E, Holmes C, Yang X, Sciare J (2011). Modeled methanesulfonic acid (MSA) deposition in Antarctica and its relationship to sea ice. *Journal of Geophysical Research* **116**, D23214. doi:10.1029/2011JD016383

Hsu SA, Meindl EA, Gilhousen DB (1994). Determining the power-law wind-profile exponent under near-neutral stability conditions at sea. *Journal of Applied Meteorology* **33**, 757–765. doi:10.1175/1520-0450(1994)033<0757:DTPLWP>2.0.CO;2

Inomata Y, Hayashi M, Osada K, Iwasaka Y (2006). Spatial distributions of volatile sulfur compounds in surface seawater and overlying atmosphere in the north-western Pacific Ocean, eastern Indian Ocean, and Southern Ocean. *Global Biogeochemical Cycles* **20**, GB2022. doi:10.1029/2005GB002518

Kettle A, Andreae M (2000). Flux of dimethylsulfide from the oceans: a comparison of updated data sets and flux models. *Journal of Geophysical Research* **105**, 26793–26808. doi:10.1029/2000JD900252

Kim I, Hahm D, Park K, Lee Y, Choi JO, Zhang M, Chen L, Kim HC, Lee S (2017). Characteristics of the horizontal and vertical distributions of dimethyl sulfide throughout the Amundsen Sea polynya. *The Science of the Total Environment* **584–585**, 154–163. doi:10.1016/J.SCITOTENV.2017.01.165

Kloster S, Feichter J, Maier-Reimer E, Six KD, Stier P, Wetzel P (2006). DMS cycle in the marine ocean–atmosphere system? A global model study. *Biogeosciences* **3**, 29–51. doi:10.5194/BG-3-29-2006

Lana A, Bell T, Simó R, Vallina SM, Ballabrera-Poy J, Kettle A, Dachs J, Bopp L, Saltzman E, Stefels J (2011). An updated climatology of surface dimethlysulfide concentrations and emission fluxes in the global ocean. *Global Biogeochemical Cycles* **25**, GB1004. doi:10.1029/2010GB003850

Lana A, Simó R, Vallina SM, Dachs J (2012). Potential for a biogenic influence on cloud microphysics over the ocean: a correlation study with satellite-derived data. *Atmospheric Chemistry and Physics* **12**, 7977–7993. doi:10.5194/ACP-12-7977-2012

Legrand M, Sciare J, Jourdain B, Genthon C (2001). Subdaily variations of atmospheric dimethylsulfide, dimethylsulfoxide, methanesulfonate, and non-sea-salt sulfate aerosols in the atmospheric boundary layer at Dumont d'Urville (coastal Antarctica) during summer. *Journal of Geophysical Research* **106**, 14409–14422. doi:10.1029/2000JD900840

Lennartz ST, Krysztofiak G, Marandino CA, Sinnhuber BM, Tegtmeier S, Ziska F, Hossaini R, Krüger K, Montzka SA, Atlas E (2015). Modelling marine emissions and atmospheric distributions of halocarbons and dimethyl sulfide: the influence of prescribed water concentration vs. prescribed emissions. *Atmospheric Chemistry and Physics* **15**, 11753–11772. doi:10.5194/ACP-15-11753-2015

Levasseur M (2011). Ocean science: if Gaia could talk. *Nature Geoscience* **4**, 351–352. doi:10.1038/NGEO1175

Lin CT, Baker AR, Jickells TD, Kelly S, Lesworth T (2012). An assessment of the significance of sulphate sources over the Atlantic Ocean based on sulphur isotope data. *Atmospheric Environment* **62**, 615–621. doi:10.1016/J.ATMOSENV.2012.08.052

Liss PS, Merlivat L (1986). Air–sea gas exchange rates: Introduction and synthesis. In 'The role of air–sea exchange in geochemical cycling'. (Ed. P Buat-Ménard) NATO ASI Series (Series C: Mathematical and Physical Sciences), Vol 185, pp. 113–127. (Springer: Dordrecht)

Marandino C, Tegtmeier S, Krüger K, Zindler C, Atlas E, Moore F, Bange HW (2013). Dimethylsulphide (DMS) emissions from the western Pacific Ocean: a potential marine source for stratospheric sulphur? *Atmospheric Chemistry and Physics* **13**, 8427–8437. doi:10.5194/ACP-13-8427-2013

Millero FJ, Sohn ML (1992). 'Chemical oceanography.' (CRC Press: Boca Raton, FL)

Nightingale PD, Malin G, Law CS, Watson AJ, Liss PS, Liddicoat MI, Boutin J, Upstill-Goddard RC (2000). In situ evaluation of air-sea gas exchange parameterizations using novel conservative and volatile tracers. *Global Biogeochemical Cycles* **14**, 373–387. doi:10.1029/1999GB900091

Park KT, Lee K, Yoon YJ, Lee HW, Kim HC, Lee BY, Hermansen O, Kim TW, Holmén K (2013). Linking atmospheric dimethyl sulfide and the Arctic Ocean spring bloom. *Geophysical Research Letters* **40**, 155–160. doi:10.1029/2012GL054560

Park KT, Jang S, Lee K, Yoon YJ, Kim MS, Park K, Cho HJ, Kang JH, Udisti R, Lee BY (2017). Observational evidence for the formation of DMS-derived aerosols during Arctic phytoplankton blooms. *Atmospheric Chemistry and Physics* **17**, 9665–9675. doi:10.5194/ACP-17-9665-2017

Park KT, Lee K, Kim TW, Yoon YJ, Jang EH, Jang S, Lee BY, Hermansen O (2018). Atmospheric DMS in the Arctic Ocean and its relation to phytoplankton biomass. *Global Biogeochemical Cycles* **32**, 351–359. doi:10.1002/2017GB005805

Preunkert S, Legrand M, Jourdain B, Moulin C, Belviso S, Kasamatsu N, Fukuchi M, Hirawake T (2007). Interannual variability of dimethylsulfide in air and seawater and its atmospheric oxidation by-products (methanesulfonate and sulfate) at Dumont d'Urville, coastal Antarctica (1999–2003). *Journal of Geophysical Research* **112**, D06306. doi:10.1029/2006JD007585

Preunkert S, Jourdain B, Legrand M, Udisti R, Becagli S, Cerri O (2008). Seasonality of sulfur species (dimethyl sulfide, sulfate, and methanesulfonate) in Antarctica: inland versus coastal regions. *Journal of Geophysical Research* **113**, D15302. doi:10.1029/2008JD009937

Quinn P, Bates T (2011). The case against climate regulation via oceanic phytoplankton sulphur emissions. *Nature* **480**, 51–56. doi:10.1038/NATURE10580

Read K, Lewis A, Bauguitte S, Rankin AM, Salmon R, Wolff EW, Saiz-Lopez A, Bloss W, Heard D, Lee J (2008). DMS and MSA measurements in the Antarctic Boundary Layer: impact of BrO on MSA production. *Atmospheric Chemistry and Physics* **8**, 2985–2997. doi:10.5194/ACP-8-2985-2008

Saltzman ES, King DB, Holmen K, Leck C (1993). Experimental determination of the diffusion coefficient of dimethylsulfide in water. *Journal of Geophysical Research* **98**, 16481–16486. doi:10.1029/93JC01858

Sciare J, Mihalopoulos N, Dentener F (2000). Interannual variability of atmospheric dimethylsulfide in the southern Indian Ocean. *Journal of Geophysical Research* **105**, 26369–26377. doi:10.1029/2000JD900236

Simo R, Dachs J (2002). Global ocean emission of dimethylsulfide predicted from biogeophysical data. *Global Biogeochemical Cycles* **16**, 26-1–26-10. doi:10.1029/2001GB001829

Tortell P, Gueguen C, Long M, Payne C, Lee P, DiTullio G (2011). Spatial variability and temporal dynamics of surface water pCO_2, $\Delta O_2/Ar$ and dimethylsulfide in the Ross Sea, Antarctica. *Deep-Sea Research. Part I, Oceanographic Research Papers* **58**, 241–259. doi:10.1016/J.DSR.2010.12.006

Tortell PD, Long MC (2009). Spatial and temporal variability of biogenic gases during the Southern Ocean spring bloom. *Geophysical Research Letters* **36**, L01603. doi:10.1029/2008GL035819

Tortell PD, Long MC, Payne CD, Alderkamp AC, Dutrieux P, Arrigo KR (2012). Spatial distribution of pCO_2, $\Delta O_2/Ar$ and dimethylsulfide (DMS) in polynya waters and the sea ice zone of the Amundsen Sea, Antarctica. *Deep-Sea Research. Part II, Topical Studies in Oceanography* **71–76**, 77–93. doi:10.1016/J.DSR2.2012.03.010

Vallina SM, Simó R, Gassó S (2006). What controls CCN seasonality in the Southern Ocean? A statistical analysis based on satellite-derived chlorophyll and CCN and model-estimated OH radical and rainfall. *Global Biogeochemical Cycles* **20**, GB1014. doi:10.1029/2005GB002597

Vogt M, Liss P (2009). Dimethylsulfide and climate. *Geophysical Monograph* **187**, 197–232.

von Glasow R, Crutzen P (2004). Model study of multiphase DMS oxidation with a focus on halogens. *Atmospheric Chemistry and Physics* **4**, 589–608. doi:10.5194/ACP-4-589-2004

Wanninkhof R (1992). Relationship between wind speed and gas exchange. *Journal of Geophysical Research* **97**, 7373–7382. doi:10.1029/92JC00188

Xu G, Gao Y, Lin Q, Li W, Chen L (2013). Characteristics of water-soluble inorganic and organic ions in aerosols over the Southern Ocean and coastal East Antarctica during austral summer. *Journal of Geophysical Research* **118**, 13303–13318. doi:10.1002/2013JD019496

Yan J, Jung J, Zhang M, Xu S, Lin Q, Zhao S, Chen L (2019). Significant underestimation of gaseous methanesulfonic acid (MSA) over Southern Ocean. *Environmental Science & Technology* **53**, 13064–13070. doi:10.1021/ACS.EST.9B05362

Yang GP, Zhang HH, Su LP, Zhou LM (2009). Biogenic emission of dimethylsulfide (DMS) from the North Yellow Sea, China and its contribution to sulfate in aerosol during summer. *Atmospheric Environment* **43**, 2196–2203. doi:10.1016/J.ATMOSENV.2009.01.011

Zhai X, Li J-L, Zhang H-H, Tan D-D, Yang G-P (2019). Spatial distribution and biogeochemical cycling of dimethylated sulfur compounds and methane in the East China Sea during spring. *Journal of Geophysical Research. Oceans* **124**, 1074–1090. doi:10.1029/2018JC014488

Zhai X, Song Y-C, Li J-L, Yang J, Zhang H-H, Yang G-P (2020). Distribution Characteristics of dimethylated sulfur compounds and turnover of dimethylsulfide in the northern South China Sea during summer. *Journal of Geophysical Research: Biogeosciences* **125**, e2019JG005363. doi:10.1029/2019JG005363

Zhang M, Chen L (2015). Continuous underway measurements of dimethyl sulfide in seawater by purge and trap gas chromatography coupled with pulsed flame photometric detection. *Marine Chemistry* **174**, 67–72. doi:10.1016/J.MARCHEM.2015.05.006

Zhang M, Chen L, Xu G, Lin Q, Liang M (2015). Linking phytoplankton activity in polynya and sulfur aerosols at Zhongshan station, East Antarctica. *Journal of the Atmospheric Sciences* **72**, 4629–4642. doi:10.1175/JAS-D-15-0094.1

Zhang M, Marandino CA, Chen L, Sun H, Gao Z, Park K, Kim I, Yang B, Zhu T, Yan J, Wang J (2017). Characteristics of the surface water DMS and pCO_2 distributions and their relationships in the Southern Ocean, southeast Indian Ocean, and northwest Pacific Ocean. *Global Biogeochemical Cycles* **31**, 1318–1331. doi:10.1002/2017GB005637

Handling Editor: Ying Chen